

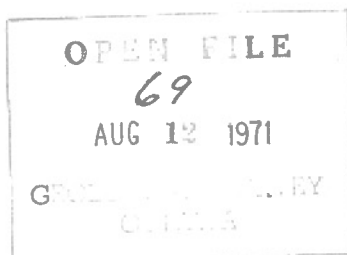
Microprobe Analyses of Pyroxenes, and Chemical
Analyses, Norms, and Modes of Nipissing Diabase
from Henwood Township, Ontario.

J.L. Jambor

Geological Survey of Canada, Ottawa

This document was produced
by scanning the original publication.

Ce document est le produit d'une
numérisation par balayage
de la publication originale.



Introduction

This report contains supplementary tables and descriptive data to accompany the writer's paper on The Nipissing Diabase. The paper is to be published in volume 11, part 1, of the Canadian Mineralogist, which is a special issue on The Silver-Arsenide Deposits of the Cobalt-Gowganda Region, Ontario. Figure numbers in the present report correspond to those given in the paper in the Canadian Mineralogist.

Appendix 1 - Pyroxene Compositions

Microprobe analyses of pyroxenes from the Henwood township diabases are shown in Figures 20 to 25. Appendix 1 consists of brief descriptive notes of the analyzed grains.

Appendix 2 - Chemical Analyses

Chemical analyses and norms of 18 rocks from the Henwood Lower sheet are given in Table A2-1. Analyses and norms of 32 rocks from the overlying diabase basin (Upper sheet and the Flank section) are given in Tables A2-2 and A2-3. The analytical methods and accuracy of the data are described in detail by Eade and Fahrig (1971) and need not be repeated here.

Variations of the oxides in the intrusions are shown in Figures 26 and 27. Modal analyses, by D.G. Fong, of the Upper sheet and Flank are shown in the final figure (as this was not shown in the original paper, no figure number is given). The modes should be regarded as reconnaissance analyses as they are for the most part based on only 1000 to 1500 counts per thin section.

References:

Eade, K.E., and Fahrig, W.F.

- 1971: Geochemical evolutionary trends of continental plates - a preliminary study of the Canadian Shield, Geol. Surv. Canada Bull. 179.

Jambor, J.L.

- 1971: The Nipissing diabase, Canad. Mineral., 11, pt. 1 (in press)

Appendix 1

Notes to accompany Figures 20 to 25 showing microprobe compositions of the pyroxenes from the upper sheet and flank section of the Henwood diabase basin.

Upper Sheet

Top contact at footage 1671.

Footage 1701: Upper quartz diabase; augite, pigeonite, inverted pigeonite.

Grain 1: Extensively altered grain 1 x 0.6 mm with fresh central portion 0.5 x 0.25 mm consisting of normal pigeonite. Grain 2: Augitic clinopyroxene with grain margins slightly zoned, but extensively replaced by greenish biotite and bluish-green amphibole. Analysis on unaltered core area. Grain 3: Normal twinned clinopyroxene without zoning. Grain 4: Normal augitic clinopyroxene. Grain 5: Core (5-2) and rim (5-1) of zoned clinopyroxene grain with rim showing higher birefringence. Adjacent grain gave Wo 39 En 47 (not plotted). Grain 6: Zoned clinopyroxene, with analysis 6-1 on core and 6-2 on rim. Some parts of the grain appear to contain micron-sized lamellae. Grain 7: Clinopyroxene in contact with 6-2. No lamellae visible. Grain 8: Zoned clinopyroxene without exsolution lamellae. Analysis 8 on core, 8-2 on higher-birefringent rim. One side of the grain has a partial rim of a second clinopyroxene with irregular, pebbly relief and birefringence (8-3).

Footage 1826: varied texture zone; augite, inverted pigeonite. Grain 1: Augitic clinopyroxene, twinned, needle-like with length 1.5 mm but with terminal parts pseudomorphed by amphibole. Analysis 1-1 represents the fresh central part of the grain. An interior patch and one edge of the crystal have the appearance of inverted pigeonite except that calcium rich lamellae are absent; rather, the high-calcium material is an almost continuous sheet of blebs which give the grain a pebbly surface. Microprobe analysis of the calcium-rich part falls at point 1-2, whereas that of the sparse calcium-poor material falls at 1-3. The Wo content of 1-3 may be high because of interference from the associated calcium-rich clinopyroxene. Grain 2: Clinopyroxene, surrounded by an alteration rim containing abundant amphibole. Grain 3: Ordinary augite. Grain 4: Ordinary augite partly mantled by pigeonite which subsequently inverted. The latter contains well-defined calcium-rich lamellae in an orthopyroxene host which has been very extensively replaced

by amphibole. Grain 5: Inverted pigeonite similar to 4 above and in contact with it. Analyses 5-1 and 5-2 represent the calcium-rich and calcium-poor portions of fresh residual patches of the inverted pigeonite. Analyses 5-3 and 5-4 are the equivalent phases in a turbid area partly replaced by amphibole. (See Figure 23 for a better quantitative estimate of the composition of the orthopyroxene host in such material). Grain 6: Zoned clinopyroxene with rim having higher birefringence and higher iron content. Microprobe scans indicate that sub-micron exsolution lamellae are present throughout the grain. Only clinopyroxene was detected on an X-ray diffraction pattern made on part of the grain.

Footage 1850: hypersthene-bearing, lower part of varied-texture zone; orthopyroxene, augite, inverted pigeonite. Grain 1: large zoned grain of orthopyroxene with most of it being of core composition (1-1) and with rim iron-rich (1-2). Part of the grain is mantled by inverted pigeonite with narrow calcium-rich lamellae, but a few coarser blebs and worm-like rods also occur in the orthopyroxene near its margins. Microprobe analysis of the worm-like rods gave Wo 39 En 46 (same as point 9-2). Grain 2: Inverted pigeonite partly mantled by iron-rich orthopyroxene. Most of the grain consists of diffuse calcium-rich lamellae in a turbid orthopyroxene host for which analysis 2-3 was obtained (identification confirmed by X-ray powder pattern; the higher-than-normal calcium is probably attributable to interference from the calcium-rich exsolved phase). A few clear patches of inverted pigeonite are scattered within the main turbid grain; microprobe analysis of one of these near the core is represented by point 2-1. The iron-rich orthopyroxene rim (2-2) is free of lamellae; although the rim and inverted main turbid grain extinguish together and have irregular, apparently gradational boundaries, the rim does not appear to be inverted material. Summary: Iron-rich orthopyroxene (2-2) probably molded on pigeonitic clinopyroxene which subsequently inverted to orthopyroxene (2-1, 2-3) with exsolved calcium-rich lamellae. Grain 3: Isolated L-shaped grain with maximum length 0.5 mm; similar to 2-2, but not in intimate association with another pyroxene. One portion of the grain contains myrmekitic augite; the other portion represented by point 3 is free of augite. Grain 4: Inverted pigeonite with orthopyroxene host (4-1) and calcium-rich clinopyroxene lamellae (4-2). Grain 5: Ordinary clinopyroxene, Wo 42 En 41 (not plotted). Grains 6, 7:

Clinopyroxene. Grain 8: Zoned clinopyroxene with iron-rich rim of higher birefringence. Grain 9: Inverted pigeonite with host 9-1 (Wo 5, En 49, not shown) and calcium-rich lamellae 9-2.

Footage 1945: hypersthene diabase zone; orthopyroxene, augite, inverted pigeonite. Grain 1: Large zoned orthopyroxene grain with magnesium-rich core (1-1) and iron-rich rim (1-2). Myrmekitic blebs of augite are abundant in most, but not all, of the rim. Grain 2: Inverted pigeonite with well-defined calcium-rich lamellae in herringbone arrangement in an orthopyroxene host, the latter being point 2. Grain 3: Similar to 2 above. Analysis 3-1 represents orthopyroxene host and 3-2 exsolved lamellae. Grains 4,5,6,7,8: Normal clinopyroxenes.

Footage 2201: hypersthene diabase zone; orthopyroxene, augite, inverted pigeonite rims on orthopyroxene. Grain 1: Zoned orthopyroxene with analysis 1-1 on core and 1-2 on rim. Myrmekitic blebs of augite are abundant near the margins of most of the grain. Analysis made on an area free of blebs. Grain 2: Orthopyroxene similar to 1 above. Grain 3: Orthopyroxene rim on part of a large grain approximately 1 x 2 mm. Much of grain contains blebs of augite and in a few patches well-defined lamellae are present. All parts of the orthopyroxene host uniformly extinguish and show uniform zoning regardless of whether blebs and lamellae are present or absent. Lamellae are not parallel to the principal crystallographic directions of the orthopyroxene core, suggesting that originally the core was mantled by pigeonite which subsequently inverted. Grains 4,5,6: Typical calcium-rich clinopyroxenes.

Footage 2301: hypersthene diabase zone; orthopyroxene, augite, inverted pigeonite rims on orthopyroxene. Grains 1: Irregular grain of orthopyroxene, predominantly iron-rich (1-2) with less birefringent core (1-1). Augitic blebs are abundant at the margins of part of the grain. A spot analysis on one bleb gave 18.7% CaO. Grain 2: Large orthopyroxene grain similar to 1 above, but with most of the grain magnesium-rich (2-1). Some well-defined lamellae occur in patches at the grain margins. The orientation of the lamellae is inclined with respect to the orthopyroxene, and the angle of inclination is not uniform in all patches. Grain 3: Twinned clinopyroxene with herringbone

cleavage simulating fine lamellae. Microprobe scans show that lamellae are absent. Grain 4: Same as 3 above. Grain 5: Zoned clinopyroxene with higher birefringent rim. Microprobe readings at intermediate positions on the grain confirm that the high-calcium core follows the trend as shown: 5-1: core; 5-2: intermediate position; 5-3: rim. Note the similarity of the initial trend with that of grain 8, footage 2475. Grain 6: Zoned clinopyroxene with analysis 6-1 on core, 6-2 near rim, and 6-3 on extreme rim near grain boundary. The compositional trend follows the same path as the outer part of grain 5 above.

Footage 2419: basal quartz diabase; augite, pigeonite, inverted pigeonite.

Grain 1: Well-zoned pigeonitic clinopyroxene with maximum extent of iron-enrichment in rim not determinable because of alteration. About 75 per cent of the grain is magnesium-rich (1-1), with a continuous but relatively abrupt rise in iron content at the rim (1-2). Lamellae are absent. Grain 2: Iron-rich edge of a zoned pigeonite grain with most of the magnesium-rich core containing minute blebs of lower-birefringent material (orthopyroxene?) slightly elongated parallel to (110) cleavage and giving a mottled appearance under crossed nicols. Grain 3: Zoned inverted pigeonite with asymmetrical zoning and herringbone augitic lamellae. Most of the orthopyroxene has a compositional range from 3-1 to 3-2. A narrow iron-rich zone (3-3) is present at one edge of the crystal where it is in contact with quartz. The higher-than-normal calcium value for this point is due to interference from augitic lamellae. Grain 4: Representative clinopyroxene. Most grains are similar to those occurring in the roof quartz diabase.

Footage 2475: basal quartz diabase; orthopyroxene, augite, pigeonite.

Grain 1: Large orthopyroxene grain 1.0 x 0.5 mm, with only a few patches of fresh material remaining. Grain 2: Pigeonite grain, largely mantled by a narrow rim of zoned augitic clinopyroxene (3). Grain 3: Clinopyroxene rim around pigeonite (2). Analysis 3-1 is on the inner rim in contact with the pigeonite and 3-2 on the exterior rim. Grain 4: Pigeonite adjacent to (2) above and in optical continuity with it, but not mantled by augite. Grains 5,6: Normal clinopyroxenes. Grain 7: Zoned clinopyroxene with 7-1 on core and 7-2 on rim. Grain 8: Asymmetrically zoned clinopyroxene with irregular segmented extinction simulating strain effects. Analysis 8-1 is from the core, and 8-2 from the higher birefringent rim.

Flank Section of the Upper Diabase Basin

HF-3: near bottom of sheet; transitional hypersthene diabase; orthopyroxene, augite, inverted pigeonite. Grain 1: Orthopyroxene core, part of a large grain mantled by inverted pigeonite. Grain 2: Zoned inverted pigeonite with 2-1 representing the core of the orthopyroxene host, and 2-2 the rim. The exsolved clinopyroxene lamellae are extremely fine and may be of augite rather than the low-calcium compositions indicated by points 2-3 (core) and 2-4 (rim). Grains 3,4: Ordinary clinopyroxenes. Grain 5: Calcium-rich clinopyroxene, with analysis 5-1 on the core and 5-2 on the rim.

HF-6: lower part of varied-texture zone; augite, inverted pigeonite. Grain 1: Core (1) and iron-rich rim of zoned clinopyroxene grain. Grains 2, 3: Normal clinopyroxenes.

HF-11: varied-texture diabase; augitic clinopyroxene, pigeonite, inverted pigeonite. Grain 1: Zoned clinopyroxene, pigeonitic, with most of grain having inverted to orthopyroxene plus exsolved augite. The orthopyroxene host is extensively altered and turbid. Analysis 1-1 in from the core position of the univerted pigeonite, and 1-2 the rim. Grain 2: Composite twinned grain consisting of a high-calcium clinopyroxene (open square 1) forming an unaltered spine along the (100) twin plane. Most of the marginal portion surrounding the spine is altered inverted pigeonite, but one end of the crystal is relatively fresh and consists of magnesium-rich pigeonite (open square 2) at the twin plane, and zoned inverted pigeonite progressively more iron-rich toward the exterior of the grain. Analyses 2-3 and 2-4 of the inverted pigeonite are calcium-rich because of interference from (001) lamellae of augite. Summary: high-calcium clinopyroxene core (1) mantled by pigeonite, (2) the marginal parts (2-3, 2-4) having inverted to orthopyroxene plus augite. Grain 3: Zoned clinopyroxene, with analysis 3 on core and iron-rich analysis on rim. Grains 4,5, 6,7: Zoned clinopyroxenes, as above.

HF-12: upper quartz diabase zone close to varied-texture zone. Grain 1: Pigeonite grain, zoned, with analysis 1-1 on core and 1-2 on rim. Grain 2: Pigeonite grain molded onto a large clinopyroxene crystal represented by point 4. Grain 3: Pigeonite grain molded onto zoned clinopyroxene (point 5). Grain 4: See 2 above. Grain 5: Zoned clinopyroxene. Grain 6: Zoned clinopyroxene with analysis at core (6-1), intermediate position, and rim (6-2). Grain 7: Zoned clinopyroxene, with analysis 7-1 on core and 7-2 on rim. Grain 8: Zoned clinopyroxene twin with analysis 8-1 and 8-2 representing the core and rim respectively of one twin unit, and 8-3 the

core of the other unit. The grain is at the edge of the thin section, with the outermost rim having been cut away. Analysis 8-4 is the iron-rich remnant closest to the original rim. See also Figures 24 and 25 for zoned clinopyroxenes from this sample. Note: The position of this sample is probably closer to HF-13 and the top contact than was estimated in the field. In thin section there is textural evidence of rapid cooling.

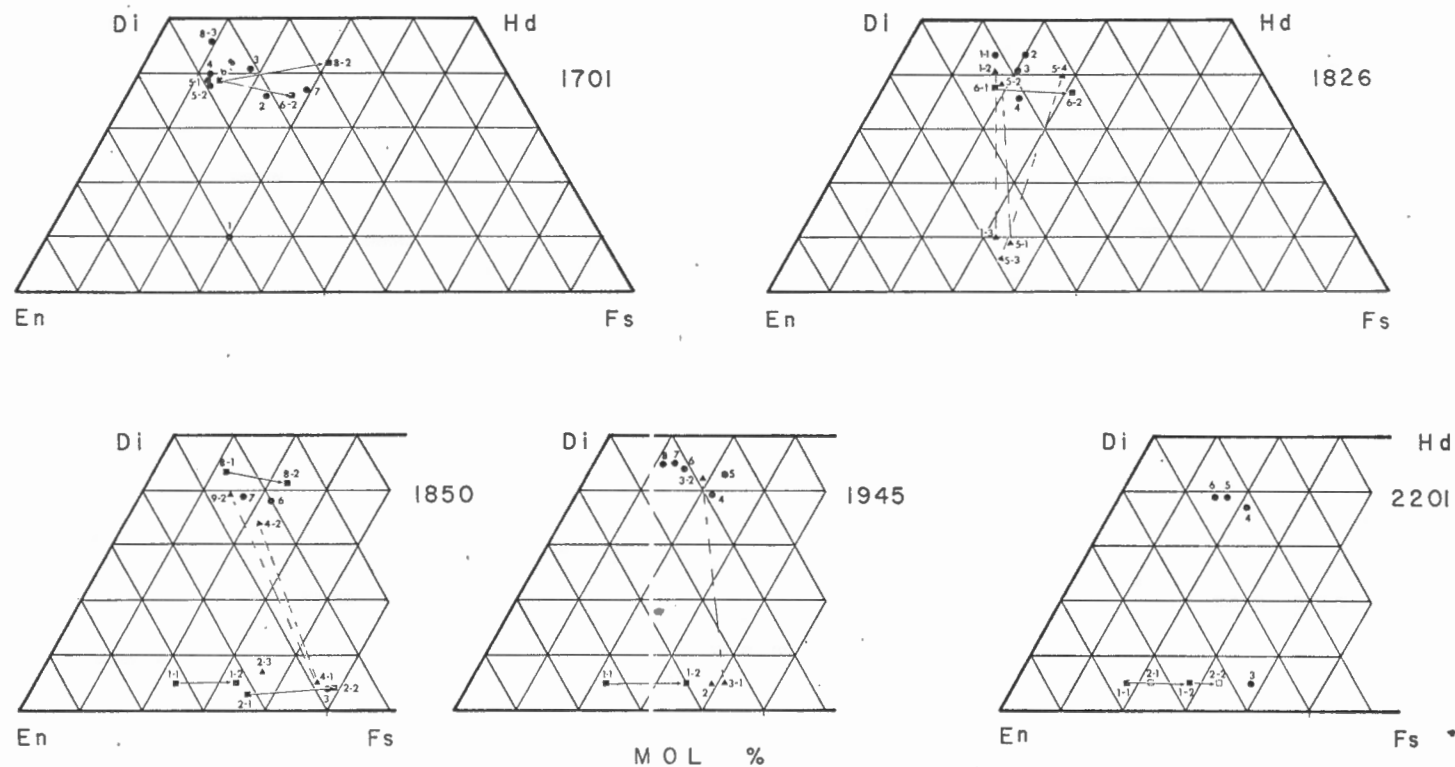


FIG. 20. Microprobe compositions of pyroxenes in the Henwood Upper sheet. Each quadrilateral contains the analyses from a single thin section. Sample 1701: upper quartz diabase; 1826 and 1850: varied-texture zone; 1945 and 2201: hypersthene diabase. Solid lines show zoned grains, with arrows pointing toward the rims. In grains with calcium-rich exsolution, the host and exsolved phases are shown as triangles joined by dashed lines. Other symbols are used only for graphical clarity.

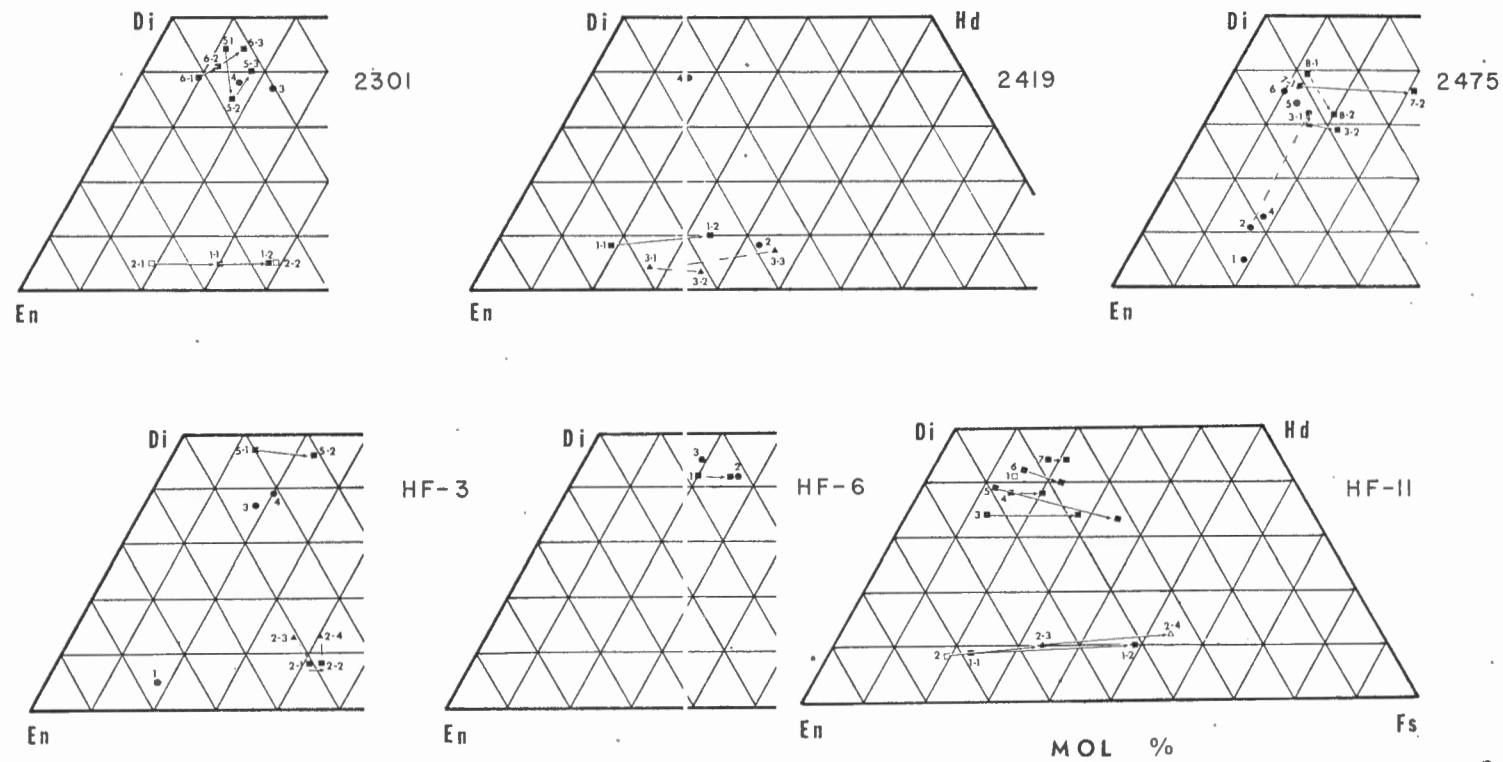


FIG. 21. Microprobe compositions of pyroxenes in the Henwood Upper sheet and Flank. Sample 2301: hypersthene diabase; 2419 and 2475: basal quartz diabase; HF-3: transitional hypersthene diabase of the Flank section; HF-6 and HF-11: varied-texture diabase. Symbols are as given in Figure 20.

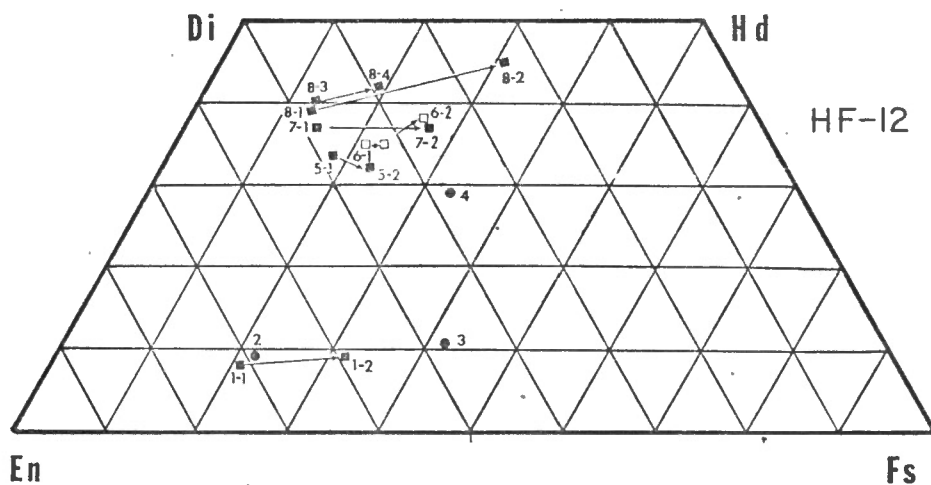


FIG. 22. Microprobe compositions of pyroxenes in the roof quartz diabase of the Henwood Flank. Solid lines with arrows show composition variations from cores to rims. Grains 1, 2, and 3 are pigeonites.

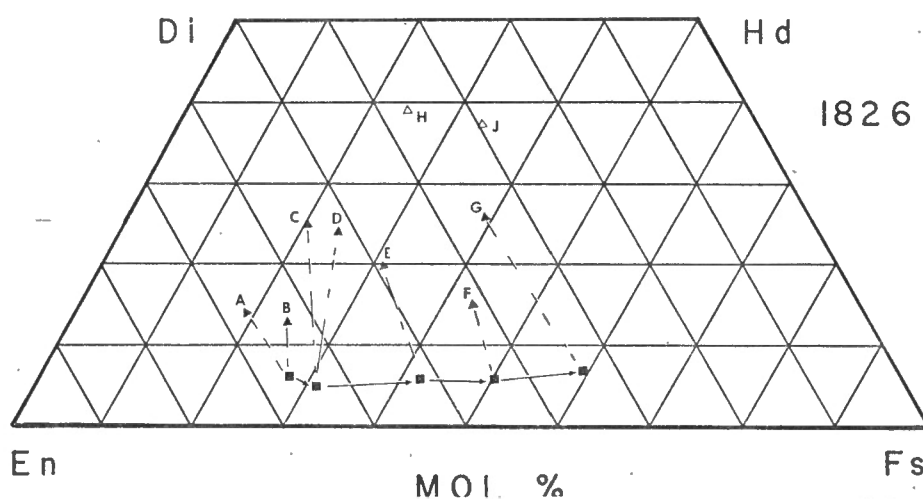


FIG. 23. Zoned inverted pigeonite in section 1826 from the lower part of the varied-texture zone in the Henwood Upper sheet. Squares denote the zoned orthopyroxene host and triangles the adjacent exsolution lamellae. The lamellae may be more calcium-rich than shown, but their thinness has prevented their complete resolution. The most calcium-rich lamellae found in the grain are shown as open triangles H and J.

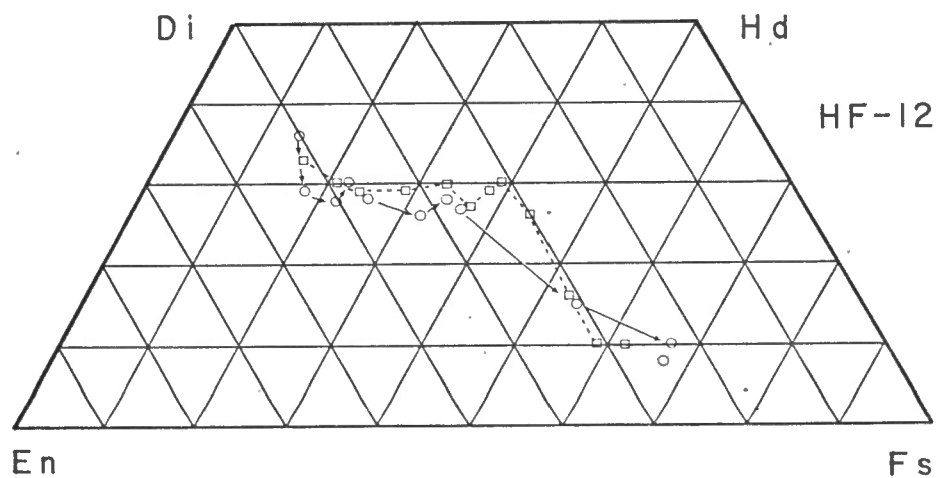


FIG. 24. Composition ranges of two grains of zoned clinopyroxene from section HF-12 (roof quartz diabase of the Henwood Flank). One grain is shown as open circles and the other as open squares.

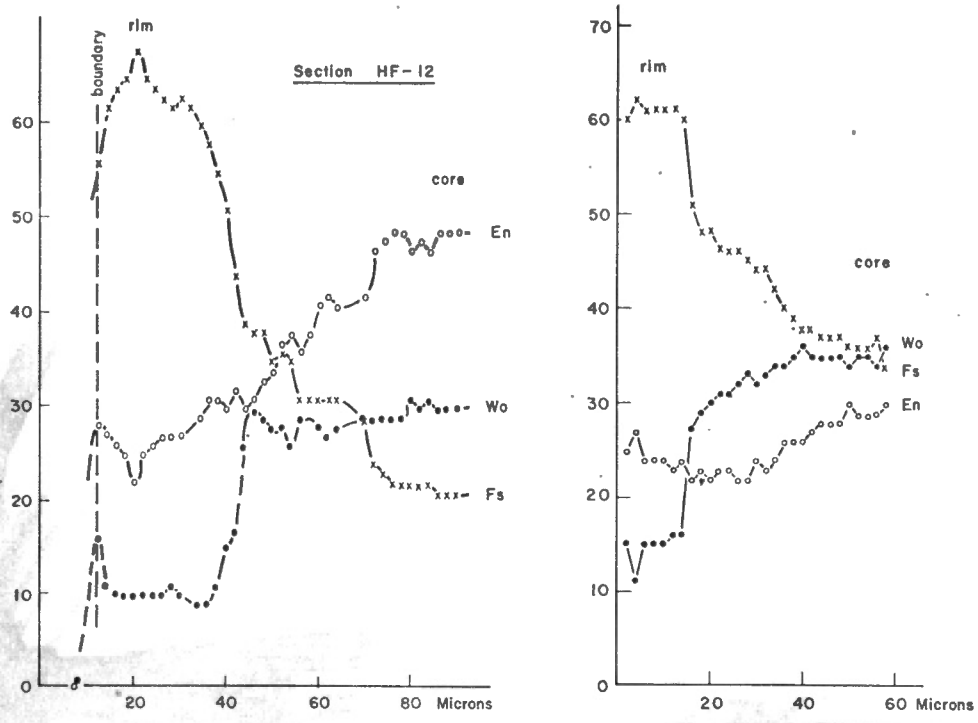


FIG. 25. Microprobe traverses showing the composition variation (atomic %, vertical scale) in two zoned grains of clinopyroxene in section HF-12. In both cases a rapid change occurs from about Wo 15 to Wo 25.

APPENDIX 2

Table A7-1, Part 1. Chemical analyses of the Lower diabase sheet, Honwood township.

No.	Quartz Diabase			Varied-Texture Diabase					
	6186	6222	6259	6293	6320	6325	6354	6384	6438
Wt. %									
SiO ₂	50.6	51.0	51.9	50.7	51.3	55.7	51.4	50.2	50.8
Al ₂ O ₃	15.3	14.1	14.7	14.6	15.1	14.9	15.2	14.8	15.1
Fe ₂ O ₃	2.1	2.5	1.7	1.2	1.2	1.4	1.7	1.3	<0.1
FeO	7.9	9.0	10.0	10.7	9.1	9.9	8.2	8.4	10.6
MnO	0.16	0.19	0.19	0.21	0.16	0.17	0.17	0.16	0.16
MgO	6.8	6.2	6.0	5.9	6.5	3.7	6.8	7.1	7.7
CaO	10.0	9.9	9.8	9.2	9.9	5.7	10.5	9.8	6.7
Na ₂ O	1.7	2.0	2.1	2.4	2.2	3.6	2.1	2.0	3.5
K ₂ O	1.2	0.9	0.9	1.0	0.7	0.9	1.1	1.4	1.0
TiO ₂	0.80	0.89	0.91	0.97	0.88	1.14	0.70	0.65	0.70
P ₂ O ₅	0.06	0.07	0.07	0.07	0.08	0.19	0.05	0.05	0.05
H ₂ O ⁺	1.9	1.5	1.1	1.6	0.8	1.7	1.4	1.6	2.2
H ₂ O ⁻	0.2	0.1	0.1	0.2	0.2	0.3	0.3	0.3	0.3
CO ₂	0.1	0.1	<0.1	0.2	<0.1	0.6	0.3	0.5	0.2
Mafic index									
Mafic index	59.5	65.0	66.1	66.9	61.3	75.3	59.3	57.7	57.9
Felsic Index*									
Felsic Index*	22.5	22.7	23.4	27.0	22.7	44.1	23.9	25.8	40.2
Index**									
Index**	22.7	22.8	23.4	27.6	22.7	48.4	24.6	27.0	41.3
Fe as FeO									
Fe as FeO	9.79	11.25	11.53	11.78	10.18	11.16	9.73	9.57	10.6
Norms**									
Q	3.63	4.56	3.71	1.13	2.77	9.39	2.08	0.80	0.00
C	0.00	0.00	0.00	0.00	0.00	0.00	0.00	0.00	0.00
Or	7.35	5.51	5.42	6.12	4.26	5.52	6.67	8.69	6.16
Ab	14.90	17.51	18.08	21.01	19.17	31.56	18.22	17.76	30.84
An	31.67	27.77	28.52	27.02	30.13	22.63	29.53	28.63	23.48
Di	9.58	10.36	8.84	7.44	9.20	0.43	10.63	9.31	4.14
Hd	5.80	7.81	8.15	7.70	7.22	0.64	7.01	6.23	3.51
En	13.10	11.71	11.11	11.75	12.40	9.35	12.44	14.25	8.06
Fs	9.09	9.66	11.75	13.96	11.16	15.68	9.41	10.94	7.82
Fo	0.00	0.00	0.00	0.00	0.00	0.00	0.00	0.00	7.01
Fa	0.00	0.00	0.00	0.00	0.00	0.00	0.00	0.00	7.49
Mt	3.15	3.75	2.51	1.80	1.79	2.10	2.53	1.98	0.00
Il	1.57	1.75	1.76	1.91	1.72	2.24	1.36	1.30	1.39
Ap	0.14	0.17	0.17	0.17	0.19	0.46	0.12	0.12	0.12
Mol An / Ab+An	66.7	59.9	59.8	54.8	59.7	40.3	69.4	63.1	41.8

* Felsic index calculated with total CaO, and with CaO less Ca as CaCO₃.

** Calculated on an anhydrous basis after deduction of CaO as CaCO₃ and totaling to 100 per cent.

Sample numbers correspond to footages in the Eplett vertical drill hole.

Table A7.2, Part 1. Chemical analyses of the Upper diabase sheet, Henwood township.

Quartz Diabase			Varied - Texture Diabase								
No.	1672	1680	1684	1701	1718	1800	1821	1826	1831	1850	1882
Wt. %											
SiO ₂	55.7	52.1	52.0	50.6	50.3	50.8	49.6	48.8	52.7	49.4	50.6
Al ₂ O ₃	13.1	15.0	15.3	14.8	16.4	18.1	14.7	14.8	13.3	17.5	13.4
Fe ₂ O ₃	7.2	2.0	2.1	2.1	1.0	0.9	0.9	1.3	2.1	1.0	1.8
FeO	10.2	7.9	8.0	7.7	7.5	7.0	7.8	8.3	9.4	6.7	6.9
MnO	0.15	0.18	0.18	0.17	0.16	0.16	0.17	0.19	0.21	0.15	0.18
MgO	2.4	7.0	7.0	7.2	7.1	8.2	6.7	7.0	5.6	7.4	8.6
CaO	3.7	9.8	10.1	10.1	10.9	11.9	11.1	10.8	8.7	11.9	11.4
Na ₂ O	2.5	1.8	1.8	1.9	1.7	1.7	1.7	2.0	2.5	1.7	1.5
K ₂ O	0.5	1.7	1.3	1.5	1.4	0.9	0.9	0.8	0.8	1.1	0.8
TiO ₂	1.86	0.63	0.64	0.58	0.50	0.50	0.54	0.65	0.76	0.45	0.65
P ₂ O ₅	0.15	0.04	0.05	0.05	0.04	0.04	0.06	0.05	0.10	0.03	0.05
H ₂ O ⁺	2.2	1.3	1.3	1.3	1.4	1.2	1.3	1.5	} 2.3	0.9	} 2.9
H ₂ O ⁻	1.1	0.2	0.1	0.1	<0.1	<0.1	<0.1	<0.1		0.1	
CO ₂	1.3	0.1	<0.1	<0.1	<0.1	0.2	0.3	0.1	0.1	0.1	0.1
Mafic index											
	87.9	58.6	59.1	57.6	54.1	52.7	51.5	58.9	67.3	52.4	50.3
Felsic											
	44.8	26.3	23.5	25.2	22.1	18.0	19.0	20.6	27.5	19.0	16.8
Index *											
	60.0	26.5	23.5	25.2	22.1	18.3	19.5	20.7	27.7	19.2	16.9
Feas FeO											
	16.68	9.70	9.89	9.59	8.40	7.81	8.61	9.47	11.29	7.60	8.52
Norms **											
Q	28.46	2.86	3.41	1.08	0.00	0.80	0.32	0.35	6.34	0.00	3.41
C	5.40	0.00	0.00	0.00	0.00	0.00	0.00	0.00	0.00	0.00	0.00
Or	3.09	10.26	7.81	9.18	8.35	5.39	5.59	5.02	4.93	6.72	4.94
Ab	22.09	15.53	15.47	16.62	14.81	14.56	15.10	17.95	22.02	14.85	13.25
An	9.34	28.38	30.29	28.36	33.97	39.58	31.30	30.80	23.63	38.08	28.68
Di	0.00	10.39	10.28	12.00	10.94	9.56	12.59	12.13	8.69	11.66	16.75
Hd	0.00	6.32	6.29	6.87	6.60	5.46	6.99	8.53	7.97	6.42	7.13
En	6.24	12.96	12.94	12.98	13.21	13.46	15.60	12.07	10.49	10.93	14.59
Fs	10.43	9.03	9.08	8.51	9.15	8.82	9.93	9.73	11.03	6.91	7.12
Fo	0.00	0.00	0.00	0.13	0.00	0.00	0.00	0.00	0.00	1.17	0.00
Fa	0.00	0.00	0.00	0.10	0.00	0.00	0.00	0.00	0.00	0.81	0.00
Mt	10.90	2.96	3.09	3.15	1.49	1.32	1.37	2.00	3.17	1.50	2.73
Il	3.69	1.22	1.23	1.14	0.98	0.96	1.08	1.31	1.50	0.88	1.29
Ap	0.36	0.10	0.12	0.12	0.10	0.09	0.15	0.12	0.24	0.07	0.12
Mol $\frac{An}{Ab+An}$	28.4	63.3	64.9	61.7	68.4	71.9	66.2	61.8	50.3	70.7	67.1

* Felsic index calculated with total CaO, and with CaO less Ca as CaCO₃

** Calculated on an anhydrous basis after deduction of CaO as CaCO₃ and totaling to 100 per cent.

Sample numbers correspond to footages in the Eplett vertical drill hole.

Table A2, Part 2. Chemical analyses of the Upper diabase sheet, Honwood township.

No.	Hypersthene Diabase						Basal Quartz Diabase				
	1945	2024	2066	2125	2201	2301	2351	2419	2447	2475	2493
Wt. %											
SiO ₂	49.8	48.9	49.5	48.0	49.5	50.7	49.5	49.0	49.0	50.6	53.6
Al ₂ O ₃	17.9	19.2	17.7	16.7	16.1	15.6	15.1	16.4	17.1	15.9	16.5
Fe ₂ O ₃	1.2	0.9	1.1	1.1	1.0	0.7	1.1	1.2	1.4	1.0	2.2
FeO	6.2	5.4	5.3	6.0	6.1	6.9	7.0	6.9	6.1	7.9	9.3
MnO	0.14	0.13	0.12	0.14	0.14	0.15	0.16	0.15	0.15	0.15	0.14
MgO	7.4	7.5	8.4	8.5	8.7	9.5	10.2	8.2	7.6	7.7	6.6
CaO	12.5	12.9	13.0	12.6	12.4	11.9	11.2	11.8	12.2	11.1	2.3
Na ₂ O	1.7	1.7	1.5	1.6	1.6	1.5	1.7	1.8	1.8	1.5	2.9
K ₂ O	0.9	0.6	0.7	0.8	0.7	0.6	0.7	0.7	0.6	0.7	2.1
TiO ₂	0.40	0.32	0.30	0.36	0.38	0.40	0.42	0.50	0.52	0.58	0.79
P ₂ O ₅	0.03	0.02	0.02	<0.02	0.03	0.03	0.03	0.04	0.04	0.05	0.06
H ₂ O ⁺	0.9	0.8	0.5	0.8	0.7	0.5	0.8	1.2	2.1	1.7	4.4
H ₂ O ⁻	<0.1	<0.1	0.1	0.1	0.1	0.1	0.2	0.1	0.2	0.1	0.4
CO ₂	<0.1	<0.1	0.1	0.1	<0.1	<0.1	<0.1	<0.1	0.2	0.1	<0.1
Mafic index	50.0	45.5	43.2	45.5	44.9	44.4	44.3	49.7	49.7	53.6	63.5
Felsic	17.2	15.1	14.5	16.0	15.6	15.0	17.6	17.5	16.4	16.5	68.5
Index*	17.2	15.1	14.6	16.1	15.6	15.0	17.6	17.5	16.8	16.7	68.5
Fear FeO	7.28	6.21	6.29	6.99	7.00	7.53	7.99	7.98	7.36	8.80	11.28
Norms **											
Q	0.00	0.00	0.00	0.00	0.00	0.12	0.00	0.00	0.00	2.69	7.89
C	0.00	0.00	0.00	0.00	0.00	0.00	0.00	0.00	0.00	0.00	5.61
Or	5.42	3.46	4.25	4.94	4.28	3.62	4.26	4.28	3.69	4.27	12.87
Ab	14.65	14.74	13.01	14.15	14.01	12.95	14.81	15.75	15.83	13.07	25.43
An	39.27	44.06	40.49	37.64	35.88	34.76	32.44	35.79	38.26	35.62	11.42
Di	13.06	12.23	14.84	15.64	15.83	14.30	14.21	13.47	12.87	10.40	0.00
Hd	6.17	5.07	5.29	6.30	6.39	6.17	5.63	6.40	5.61	6.15	0.00
En	10.81	9.48	12.89	7.98	13.15	17.52	13.70	11.20	13.58	14.93	17.03
Fs	5.86	4.51	5.27	3.69	6.07	8.67	6.23	6.10	6.79	10.12	14.73
Fo	1.34	2.80	1.18	4.83	1.34	0.00	4.11	2.57	0.09	0.00	0.00
Fa	0.80	1.47	0.53	2.46	0.68	0.00	2.06	1.55	0.05	0.00	0.00
Mt	1.77	1.34	1.64	1.67	1.50	1.04	1.64	1.80	2.11	1.49	3.31
Il	0.77	0.62	0.58	0.71	0.75	0.78	0.82	0.98	1.03	1.14	1.56
Ap	0.07	0.05	0.05	0.00	0.07	0.07	0.07	0.10	0.10	0.12	0.14
Mol $\frac{An}{Ab+An}$	71.6	73.8	74.6	71.5	70.7	71.7	67.4	68.2	69.5	72.0	29.7

Table 3. Chemical analyses of the Flank (rim) section of the Henwood diabase basin.

No.	HF-13	HF-12	HF-11	HF-9	HF-10	HF-7	HF-6	HF-4	HF-3	HF-1
Wt. %										
SiO ₂	52.0	53.0	51.2	50.5	52.6	50.9	53.3	52.8	49.4	50.1
Al ₂ O ₃	14.0	14.7	13.7	14.0	13.8	13.5	14.2	14.6	16.8	16.0
Fe ₂ O ₃	2.2	1.8	2.6	<0.1	2.0	1.9	2.3	2.2	1.8	1.1
FeO	7.9	8.2	9.2	10.2	9.9	9.9	9.7	9.5	7.5	8.0
MnO	0.18	0.17	0.20	0.16	0.20	0.21	0.20	0.19	0.14	0.15
MgO	7.2	6.9	7.3	4.4	6.3	5.7	5.8	5.7	6.3	8.0
CaO	10.8	10.6	9.2	10.1	9.1	9.2	9.5	8.8	10.8	10.0
Na ₂ O	1.7	1.9	1.9	3.0	2.6	2.4	2.2	2.4	2.1	1.7
K ₂ O	0.5	0.9	1.2	1.2	1.2	1.2	0.9	1.1	0.7	1.6
TiO ₂	0.58	0.64	0.85	0.60	0.87	0.85	0.85	0.84	0.64	0.57
P ₂ O ₅	0.04	0.05	0.05	0.09	0.04	0.06	0.06	0.06	0.05	0.05
H ₂ O	2.6	2.6	1.8	3.0	2.9	2.2	2.5	2.2	2.4	3.0
CO ₂	0.2	<0.1	<0.1	0.1	0.1	0.1	0.1	<0.1	0.1	<0.1
Mafic index	58.4	59.2	61.8	78.1	65.4	67.4	67.4	67.2	59.6	53.2
Felsic index	16.9	20.9	25.2	29.4	29.5	28.1	25.8	28.5	20.6	24.8
Index	17.3	20.9	25.2	29.6	29.7	28.3	26.0	28.5	20.7	24.8
Fe as FeO	9.88	9.82	11.54	10.2	11.70	11.61	11.77	11.48	9.12	8.99
<u>Norms</u>										
Q	6.71	4.90	3.26	0.00	2.05	2.32	6.05	4.65	1.11	0.00
C	0.00	0.00	0.00	0.00	0.00	0.00	0.00	0.00	0.00	0.00
Or	3.06	5.39	7.29	7.54	7.21	7.42	5.38	6.63	4.31	9.73
Ab	14.86	16.26	16.50	26.96	22.33	21.21	16.82	20.68	18.48	14.79
An	30.06	29.26	25.98	22.51	22.78	23.52	26.50	26.29	35.73	32.18
Di	12.09	11.72	10.16	10.22	9.91	9.85	8.84	7.76	9.57	9.59
Hd	7.10	7.63	6.68	14.66	8.52	9.44	9.74	6.96	6.11	5.51
En	12.92	11.95	13.96	4.57	11.33	10.26	10.51	10.59	11.88	13.25
Fs	8.69	8.92	10.53	7.52	11.17	11.28	10.82	11.16	8.70	8.72
Fo	0.00	0.00	0.00	1.64	0.00	0.00	0.00	0.00	0.00	1.96
Fa	0.00	0.00	0.00	2.97	0.00	0.00	0.00	0.00	0.00	1.42
Mt	3.30	2.64	3.87	0.00	2.94	2.88	3.37	3.25	2.72	1.64
Il	1.14	1.23	1.66	1.21	1.68	1.69	1.63	1.63	1.26	1.11
Ap	0.10	0.12	0.12	0.22	0.09	0.15	0.14	0.14	0.12	0.12
Mol $\frac{An}{Ab+An}$	65.6	62.9	59.7	44.0	49.0	51.1	57.0	54.5	64.6	67.2

Felsic index and norms calculated as in Table 2-1. Samples HF-13 and HF-12 are roof quartz diabases; HF-3 and HF-1 are hypersthene-bearing diabase from the lower part of the cross-section.

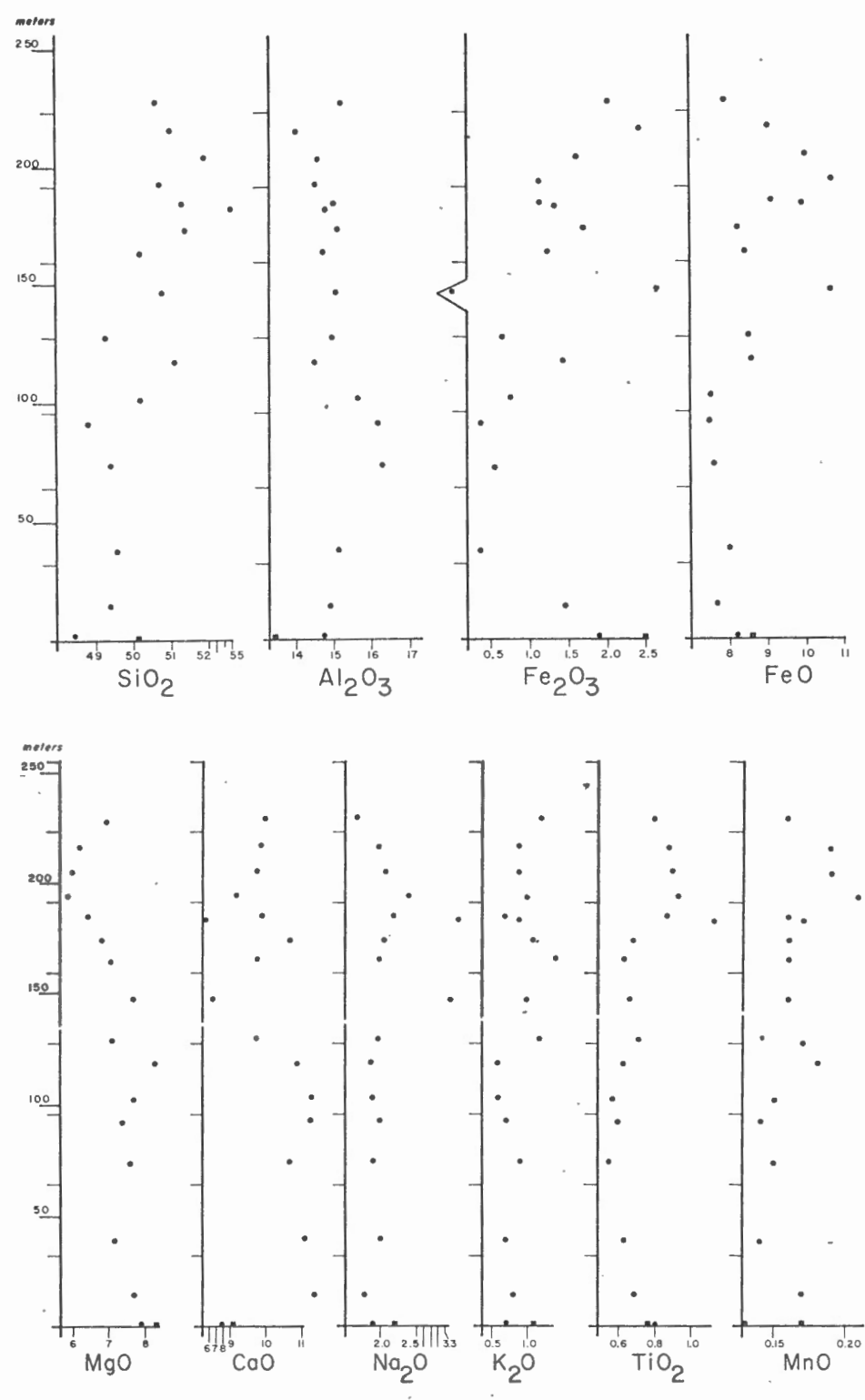


FIG. 26. Variation in weight per cent of the major oxides with height above the bottom contact of the Henwood Lower sheet. Solid squares are albitized chilled diabase at the contact. (Subsidiary vertical scale in hundreds of feet).

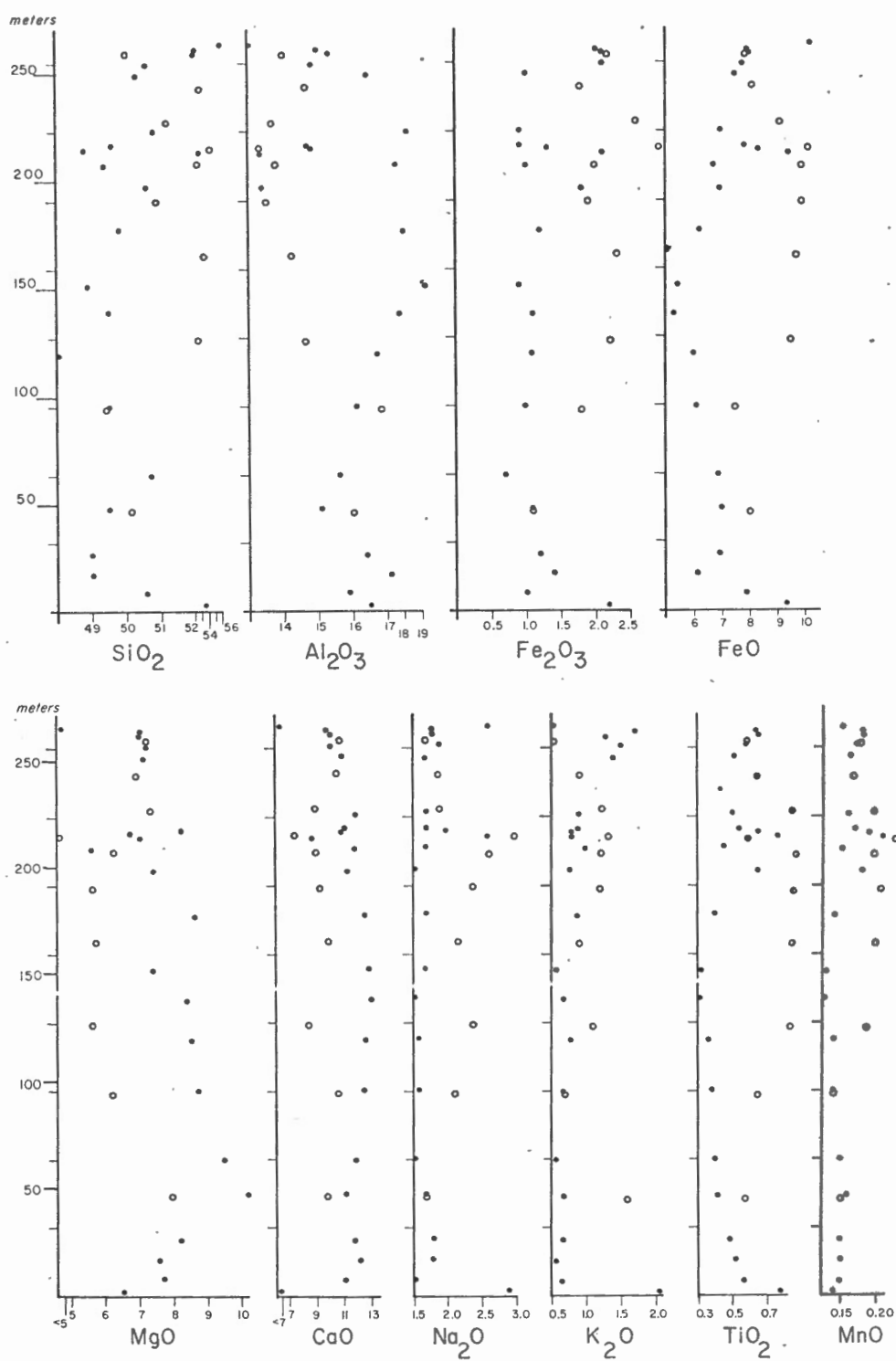
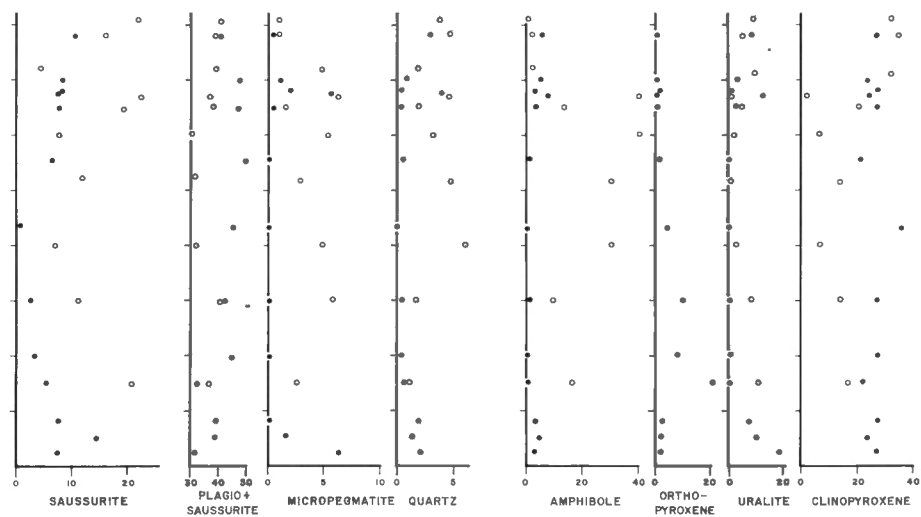


FIG. 27. Variation in weight per cent of the major oxides with height above the bottom contact of the Henwood diabase basin (the Upper sheet is shown as solid dots and the Flank as open circles; the subsidiary vertical scale is in hundreds of feet).



Modal analyses of the Henwood diabase basin, with the Upper sheet shown as dots and the Flank as open circles. The vertical scale is in hundreds of feet above the basal contact; the horizontal scale shows the volume % of the relevant minerals.

*Final figure
(see introduction)*